Research Updates

Origin of polytypism in block copolymer materials

Sangwoo Lee [1,*] Juhong Ahn [1] Liwen Chen [2] and Patryk Wąsik [3]

[1]Department of Chemical and Biological Engineering, Rensselaer Polytechnic Institute, Troy, New York 12180, USA
[2]School of Health Science and Engineering, University of Shanghai for Science and Technology, Shanghai 200093, China
[3]National Synchrotron Light Source II, Brookhaven National Laboratory, Upton, New York 11973, USA

(Received 21 August 2023; accepted 17 October 2023; published 16 November 2023)

Block copolymers have served as versatile model compounds to understand the self-assembly of inhomogeneous materials. However, the close-packed structures and relevant polytypic crystal systems in block copolymer materials still require a better understanding. In this research update, we review early and recent advancements in close-packed structures in block copolymer materials and attempts to present a framework to understand the origin of polytypism in polymeric and relevant systems. We propose a critical role of interstitial space as a structure director in polytypism and introduce the interstitial space distribution factor as a semiquantitative parameter to address the difference in the configurations of interstitial space distribution in polytypes of the same class. We also note that the random stacking of two-dimensional close-packed structures is a class of aperiodic crystals.

DOI: 10.1103/PhysRevMaterials.7.110301

I. INTRODUCTION

Packing is an important issue in everyday life. Grocers use different strategies to pack produce in various forms for better space use and customer accessibility. Integrated circuit designers pack microelectronic components tight for performance, power efficiency, and low production cost. Scientists and engineers investigate densely packed states of atoms, molecules, and mesoscale particles to understand the structure and property relationships of materials.

Spheres are often the primary geometrical choice to represent unit domains forming densely packed structures, for example, atoms, molecules, and colloidal objects, after or to approximate their shapes. The choice of spherical geometry as the unit-building domain is also partly due to the unique geometrical characteristic of spheres. Spheres have the lowest surface area density, having spherical particles the lowest surface energy density among the particles in other geometries. Therefore, self-adjustable point domains made by aggregation of inhomogeneous compounds, such as surfactants, dendrimers, and block copolymers, tend to accommodate spherical geometry [1–4]. Those spherical domains can deform to accommodate preferred long-range structures, and remarkably rich crystal structures, including quasicrystalline orders, have been reported [5–14]. However, interestingly, in the self-assembly of the spherical domains of block copolymer materials, close-packed structures are relatively scarce and have been regarded as a niche problem despite the importance of close-packing in materials and soft matter research. In this research update, we attempt to rationalize the stability of close-packed structures in the phase space of block copolymer systems and identify associated key contributions from interstitial spaces. We also discuss the potentially interesting questions for close-packed and other long-range ordered structures in block copolymer materials and beyond.

II. CLOSE-PACKED STRUCTURES OF EQUAL HARD SPHERES

Close-packed structures represent the densest packing of equal hard spheres with the volume fraction $\pi/\sqrt{18} \approx 0.74$, which has important implications in selecting stable structures. In close-packed structures, spheres have the shortest interparticle distances allowed by the particle excluded volume. Therefore, the spheres of a short-range attractive interaction such as Lennard-Jones or similar achieve the lowest potential energy state [15,16]. However, even nonattractive hard spheres with a step repulsion potential implementing the excluded volume, often referred to as athermal spheres due to the lack of crystallization heat, also prefer to form close-packed structures due to entropy. By forming the densely packed domains of athermal spheres, the whole system gains a more entropic benefit from the translational freedom of the spheres in the enlarged fluid domain, even at the expense of the reduced translational entropy of the spheres in densely packed domains [17]. This counterintuitive entropy-driven crystallization was recognized by Onsager [18] for thin-rod colloids. Thin-rod colloids form nematic orders to offer a larger space for the fluid rod particles, making a net advantage to the system. The orientational entropy of the rods in the nematic states decreases, but the increased translational entropy of the rod colloids in the freed fluid phase space increases

*lees27@rpi.edu

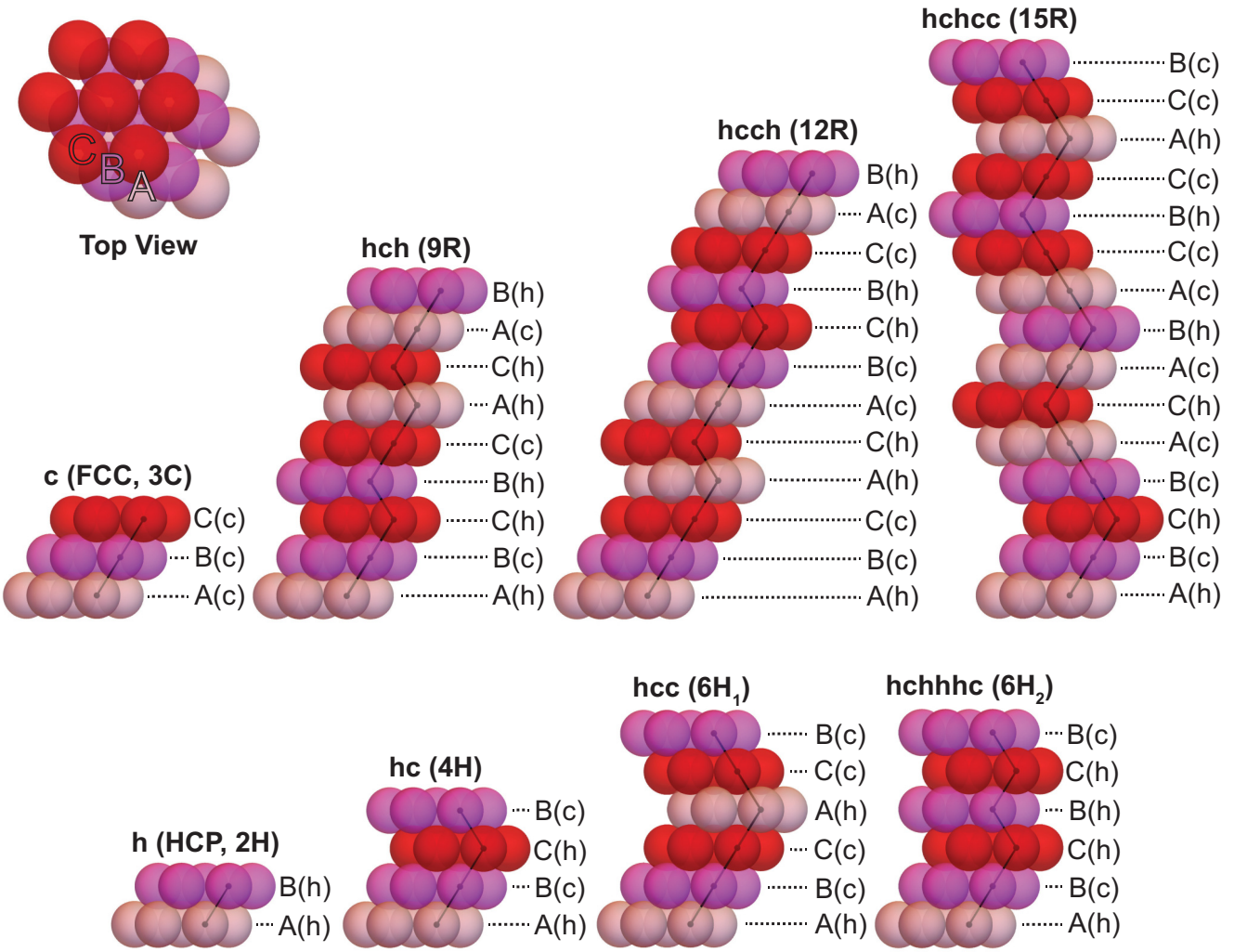

FIG. 1. Some simple stacking variants of close-packed structures of equal spheres. The A, B, and C registration sites of two-dimensional (2D) hexagonal close-packed (HCP) layers are noted in the top left panel. The registration sites and the layer stacking environment of each layer are shown on the right of each 2D-HCP layer stacking representation. The stacking environment of a layer is marked with "c" if the two nearest-neighbor layers register at different lattices and "h" if at the same. The Ramsdell notation (3C, 9R, 2H, …) is noted above the 2D-HCP layer stacking representations. In the Ramsdell notations, the prefix number indicates the number of layers in one repeating period, the letter (C, H, or R) represents cubic, hexagonal, and rhombohedral symmetry, respectively, and the subscript, if noted, is to distinguish different stacking orders of the same symmetry and stacking period [22].

the net entropy of the whole system. The entropy-driven crystallization for hard spheres was proposed by two simulation studies and experimentally verified with nearly hard-sphere colloid solutions three decades later [19–21]. Those results suggest that close-packed structures are the preferred densely packed states for thermal and athermal hard spheres. Also, close-packed structures are expected to be the first crystal structures next to the fluid phase for sufficiently hard spheres.

III. POLYTYPISM OF CLOSE-PACKED SPHERES

Close-packed structures of equal spheres are constructed by stacking two-dimensional (2D) hexagonal close-packed (HCP) lattice layers at three different registration site groups, often denoted with A, B, and C (see the top left panel in Fig. 1). The crystal structures of close-packed spheres vary with the stacking order of the 2D-HCP layers. Those close-packed structures of different crystal symmetries are referred to as polytypes, and the capability of forming polytypes by stacking one or more structurally compatible layer modules, such as 2D-HCP layers, is called polytypism, a subclass of polymorphism [23]. Close-packed structures of equal spheres are the prototypes of polytypic crystals because those structures are translatable to other polytypic crystal systems formed with the stackable layer modules registering at hexagonal layer lattice groups, such as Laves phases (see below) [24].

Since the volume fraction of close-packed equal spheres is the same, the entropically driven crystallization of spheres on any close-packed lattices generates the same degree of translational freedom to the fluid particles. However, interestingly, many colloidal systems form a specific polytype, such as

face-centered cubic (FCC) with the …ABCABC… stacking order of 2D-HCP layers or HCP with the …ABABAB… order, rather than forming a random stacking of 2D-HCP layer (RHCP) structures. This observation indicates that close-packed structures of equal spheres have different energetic states depending on a particular condition. Authors of studies using Monte Carlo methods have suggested that the FCC polytype has a slight configurational entropic advantage over other polytypes, though at most $\sim 10^{-3}\, k_B T$ per site if compared with HCP [25,26]. This preference for FCC lattices is because the ABC stacking most evenly utilizes the available 2D-HCP layer stacking lattice groups among all polytypes and the A, B, and C stacking registrations are also most evenly distributed in the crystal domain space. For example, the HCP stacking excludes a stacking registration site group in its stacking sequence only by the two other registration site groups. The entropic preference for the …ABC… stacking has explained the prevalence of FCC lattices in sufficiently large crystal domains of close-packed spherical colloids [27,28]. However, as described below, non-FCC close-packed structures in block copolymer and related systems have been reported. This observation suggests that another energetic contribution leading to non-FCC polytypes must exist and competes with the entropic advantage of FCC lattices. From the literature survey, we attempted to describe a potential origin of the non-FCC polytypes in block copolymer and related systems.

IV. CLOSE-PACKED STRUCTURES IN BLOCK COPOLYMER MELTS

Block copolymers consist of at least two chemically distinct but covalently bound polymer chains to each other, which form microphase-separated domains due to the chemical incompatibility between the different polymer chains [29]. The microphase separation provides unique dynamic, kinetic, structural, and physical properties to block copolymers, which have been the major research interests in the polymer and materials physics community over decades [30–38]. The microphase-separated domains, serving as the building constituents in the long-range ordered structures of block copolymers, are induced by increasing the segregation strength between blocks, generally gauged with χN, where χ is the interaction parameter, quantifying the chemical incompatibility between different polymer blocks, and N is the degree of polymerization of block copolymer chains. The symmetry of long-range ordered structures primarily depends on the geometry of microphase-separated domains controlled by the volume fraction of a polymer block f, which directs the preferred curvature of microphase-separated domains [39]. The representative geometries of microphase-separated domains are spheres, cylinders, sheets, and junctions of saddle curvatures [40]. Lamellar, HCP cylinders and body-centered cubic (BCC) were the long-range ordered structures recognized in the early studies of block copolymers materials [30,41], and the discovery of complex self-assembled structures, particularly three-dimensional (3D) network structures, followed [29,31,42,43]. Partly, the complexity of network structures originates from the largest dimensional freedom, i.e., 3D, in the construction of long-range ordered structures. However, although spheres are relatively simple and flexible building units for 3D self-assembly, the rich long-range orders of sphere-packing structures in block copolymer melts were not recognized until Frank-Kasper σ phases were identified from two linear block copolymer systems a decade ago [11]. Reports on long-range ordered packing structures, either on periodic or aperiodic lattices, soon followed [12,13,44–46].

Interestingly, despite the rich library of packing structures documented, close-packed structures of equal spheres, simple and universally conceivable sphere arrangements, have been relatively scarcely observed in block copolymer melts. In the early investigations of the ordered lattices by spherical domains in block copolymers, theory and experiment identified mostly BCC, and close-packed structures were barely evidenced [30,41,47,48]. Semenov [49] proposed a theoretical examination of the FCC and HCP phase domains in diblock copolymer melts based on the intermicellar potential of damping and oscillating attractive interactions over the distance of two micelles. He predicted that, as the segregation strength between the core and corona chains of spherical micelles in melts increases, the concentration of micelles increases, and the micelles form FCC first, then HCP, and finally, BCC structures. This prediction on the close-packed structure domain, sandwiched by the fluid (disordered) and BCC phase domains, was later supported by the diblock copolymer phase diagrams constructed using the self-consistent mean field theory (SCFT) calculations. However, the phase domain of close-packed structures is relatively narrow in the volume fraction parameter space, as shown in Fig. 2(a) [50,51]. The narrow stability reflects the small amount of block copolymer chains available to fill the interstitial space of close-packed spheres, relieving the packing frustration from competing for constant interface curvature and uniform thickness of microphase-separated domains [52]. In the volume fraction parameter space, the availability of the block copolymer chains in the interstitial space steeply changes, and therefore, the close-packed structure domain is stable only in a narrow domain.

The SCFT-based inspections successfully identified the phase domain of close-packed structures but provided conflicting symmetry assignments. Matsen [53] reported a slight energetic advantage of the HCP symmetry in conformationally symmetric and asymmetric diblock copolymers. However, Xie *et al.* [54] found that FCC is slightly preferred in conformationally asymmetric diblock copolymers. Due to the uncertainty, FCC is often arbitrarily assigned to the close-packed structures in diblock copolymer melts for convenience. In contrast, authors of studies on multiblock or nonlinear block copolymers reported more definitive phase assignments to close-packed structure domains, either FCC or HCP, as shown in Fig. 2(b), describing the phase diagram of the B_1AB_2C tetrablock copolymer system [42,55–58].

Experimental observations of close-packed structures in block copolymer melts had also been sporadic, but authors of recent reports made notable progress. An early experimental signature of a close-packed structure in block copolymer melt was FCC in the sheared and annealed poly(1,3-cyclohexadiene-*b*-ethylene-*co*-but-1-ene-*b*-1,3-cyclohexadiene) triblock copolymer [59]. Authors of another report on a FCC order in a diblock copolymer melt could provide only partial evidence of the FCC order.

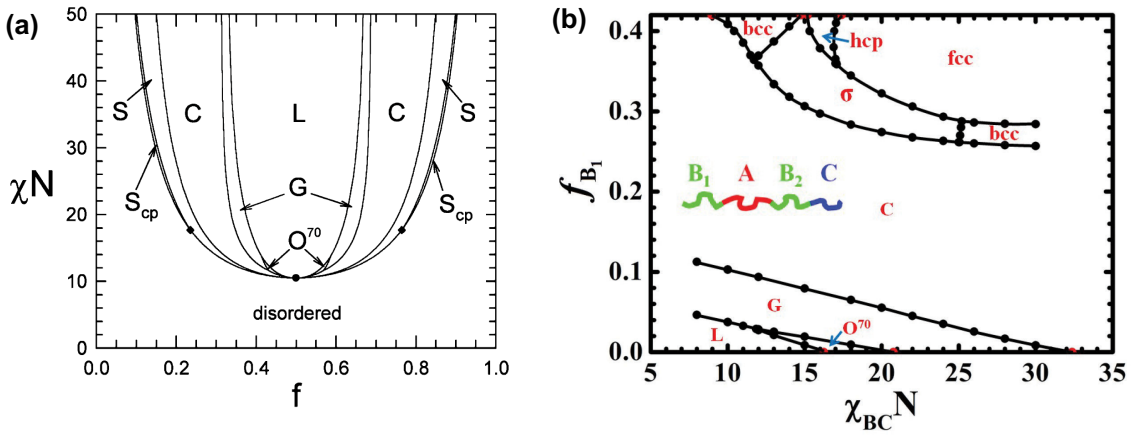

FIG. 2. Phase diagrams locating close-packed structure domains in block copolymer melts by self-consistent mean field theory (SCFT) calculations. (a) Conformationally symmetric AB diblock copolymer. The narrow close-packed structure (S_{cp}) domains are sandwiched by the disordered domain and body-centered cubic (BCC; S). The L, G, O^{70}, and C note lamellar, gyroid, *Fddd* network, and hexagonal close-packed (HCP) cylinder phase domains, respectively. Copyright 2012 American Chemical Society (Ref. [42]). (b) Conformationally symmetric B_1AB_2C tetrablock copolymer in the $\chi_{BC}N$ and f_{B_1} phase plane at $f_A = f_B = 0.42$, $f_C = 0.16$, $\chi_{AB}N = 8$, and $\chi_{AC}N = 45$. Distinct face-centered cubic (FCC) and HCP phase domains are identified at $f_{B_2} \to 0$. The σ notes Frank-Kasper σ phase. Copyright 2016 Royal Society of Chemistry (Ref. [57]).

The small angle x-ray scattering profile obtained from a poly(1,4-butadiene-*b*-ethylene oxide) (1,4-PB-PEO) sample in that report records only (111), (220), and (222) Bragg reflection peaks of FCC, and the (200) and (311) reflections are missing [60].

In contrast to the weak experimental evidence of FCC in block copolymer melts, authors of recent experimental studies have strongly confirmed the HCP structure. Hsu *et al.* [61] reported a HCP order induced by quiescent annealing of a 1,2-PB-PEO diblock copolymer cooled from a disordered state. Zhang *et al.* [62] reported HCP phases of poly(2,2,2-trifluoroethyl acrylate-*b*-2-dodecyl or 4-dodecyl acrylate-b-2,2,2-trifluoroethyl acrylate) triblock and poly(2,2,2-trifluoroethyl acrylate-*b*-4-dodecyl acrylate) diblock copolymers.

V. CLOSE-PACKED STRUCTURES IN BLOCK COPOLYMER MICELLAR COLLOIDS IN SELECTIVELY SOLVATING MEDIUM

The narrow phase domain of close-packed structures of diblock copolymer melts in Fig. 2(a) indicates a steep change in the free chain availability for partitioning in the interstitial space of close-packed block copolymer micelles. In the phase plane of diblock copolymers, as the volume fraction of a block f shifts toward a more symmetric composition from a disordered domain, the micelle concentration increases at the expense of free chains, and the spherical micelles self-assemble on close-packed lattices. As f further shifts, the interstitial space of close-packed structures cannot be filled with free chains, and the BCC phase emerges for the geometrical optimization of faceted particle domains balanced by the enthalpic and entropic competitions of polymer chains [4,49,52]. The narrow phase domain of close-packed structures of block copolymer melts can be widened using a selective medium for a block, e.g., small molecular weight solvents or relatively large polymer chains, which provides an additional suspending medium of block copolymer micellar colloids and enlarges the phase domain of close-packed structures in the volume fraction parameter space of those components.

The segregation strength between core and corona domains of block copolymer micelles is important for the stability of close-packed structures. Strong segregation between core and corona domains increases the interfacial tension, which is a steep increase of repulsion between micelles in contact because of the large penalty for the overlapping corona domains [63]. The high repulsion maintains the spherical geometry of micelles, and the packing symmetry is selected to maximize the packing volume fraction of spheres, i.e., close-packed structures [6,64]. However, block copolymer micelles are still inherently deformable. The deformability, i.e., repulsive interaction, varies with the core-corona chain incompatibility strength and solvent selectivity [65]. Weakly segregated block copolymer micelles have weaker repulsive interactions that stabilize BCC structures than close-packed lattices [16,66–68]. An exemplar system of which packing structures transit by the segregation strength, we speculate, is the thermotropic transition of BCC to FCC of poly(butylene oxide-*b*-ethylene oxide) (PBO-PEO) diblock copolymer micelles [69]. At 25 °C, the PBO-PEO diblock copolymer micelles in water order on BCC lattices, but at 52 °C, the order changes to FCC. This transition is likely driven by the increase of the segregation strength between the water-swollen PBO core and PEO corona domains by the temperature increase, as evidenced by the increased micelle size at the elevated temperatures, i.e., the hard-sphere equivalent radius of the PBO-PEO micelles, 4.6 nm at 20 °C, which increases to 5.1 nm at 30 °C and 6.1 nm at 45 °C. A similar thermotropic transition from close-packed structures to BCC but in the opposite temperature direction is observed from poly(isoprene-*b*-styrene) (PI-PS) diblock copolymer micelles of which PS block is selectively solvated in diethyl phthalate [70,71]. The PI-PS on BCC

TABLE I. Stacking variants of 2D-HCP layers forming close-packed structures in Fig. 1. For the description of notations, see the caption of Fig. 1.

Layer stacking environments	Minimum number of layers	Stacking registrations
c (FCC, 3C)	3	$[ABC]_n$
hch (9R)	9	$[ABCBCACAB]_n$
hcch (12R)	12	$[ABCACABCBCAB]_n$
hchcc (15R)	15	$[ABCBACABACBCACB]_n$
h (HCP, 2H)	2	$[AB]_n$
hc (4H)	4	$[ABCB]_n$
hcc ($6H_1$)	6	$[ABCACB]_n$
hchhhc ($6H_2$)	6	$[ABCBCB]_n$

lattices rearrange onto the lattices of FCC/HCP by cooling, which also increases the segregation strength between core and corona domains, as indicated by the size increase of micelles at the lower temperatures. We note that, although those examples show BCC-to-FCC/HCP transitions by the change in segregation strength, even strongly segregated micelles form BCC and other Frank-Kasper phases if the micelles are forced to be faceted by deprivation of selective solvents, for example, in block copolymer melts [4]. Interestingly, experimental investigators of block copolymer micelles solvated by small molecular weight solvents report both FCC and HCP structures, but the SCFT investigators of block copolymer micelles in selective homopolymers find that HCP structures are slightly more stable than FCC [72,73]. Chen *et al.* [74] documented the stability of close-packed structures using 1,2-PB-PEO diblock copolymer micelles and found that HCP is more stable than FCC. Mueller *et al.* [75] studied the packing structures of poly(ethylene oxide-*b*-2-ethylhexyl acrylate) (PEO-PEA) blended with PEO homopolymers that partition in the PEO core domains and documented a HCP phase domain. Lindsay *et al.* [76] investigated the packing structures of PS-1,4-PB diblock copolymer blended with homopolymer chains partitioning core domains and located FCC/HCP and HCP phase domains.

VI. BEYOND DICHOTOMY OF FCC AND HCP

Close-packed structures of spheres consist of stacked 2D-HCP layers, and an infinite number of crystallographically different close-packed structures are constructible by varying the stacking order of 2D-HCP layers, for example, as shown in Fig. 1 and Table I. However, for block copolymer melts and micelles in selectively solvating medium, FCC and HCP structures have been the primary crystal structures of interest, and the other polytypes are generally assumed metastable or ignored because of the close energy states of FCC and HCP and the lacking evidence supporting the other polytypes [53,54].

A reproducible non-FCC or HCP polytype documented in block copolymer micelles is RHCP, which has a nonregular stacking order of 2D-HCP layers registering at the A, B, and C sites. Park *et al.* [70] noticed RHCP structures coexisting with HCP in the phase transition between FCC and HCP of PI-PS micelles selectively solvated in diethyl phthalate. They speculated that the RHCP originates from the nearly close energy states of FCC and HCP. Chen *et al.* [74] also observed the RHCP of 1,2-PB-PEO micelles in PB homopolymers. They reported a thermotropic and continuous transition between HCP and RHCP of the 1,2-PB-PEO micelles in homopolymers. They attributed the thermotropic transition between the HCP and RHCP states to the small size of crystal domains influenced by thermal fluctuations [77]. We recently reported on a phase domain of continuously transiting close-packed structures of 1,2-PB-PEO diblock copolymer micelles in water from FCC to HCP through RHCP [78].

VII. THERMODYNAMIC STABILITY OF RHCP

RHCP has been regarded as a metastable state in nearly all cases. RHCP order was recognized in cobalt, and then numerous systems of polytypic orders by 2D-HCP lattice groups, such as xenon, ice, and colloids, are known to form RHCP orders in their diffusive and displacive phase transitions [79–83]. The frequent occurrence of RHCP orders has often been attributed to the mismatch between the crystal growth rates and the diffusivity of particles in the growing crystal [27,84]. Another explanation is the small energy difference between FCC and HCP polytypes influenced by thermal fluctuations, which become more pronounced in small crystal domains [25,26,85]. Below, we discuss an explanation of the stability of RHCP.

The experimental confirmation of the entropic advantage of FCC among close-packed structures has been primarily sought using model athermal and nearly hard-sphere colloids [27,86,87]. Those colloidal systems are designed to suppress short-range attractive interactions by matching the refractive indices of colloid and suspending medium, i.e., suppressing the van der Waals interactions and adding kinetic stability with short alkylchains tethered on the surface of colloids. Those nearly hard spheres form RHCP in small crystal domains, but FCC becomes the dominant lattice configuration once the crystal domains grow large enough.

We realized that strongly segregated block copolymer micelles also could serve as nearly athermal spherical colloids by enhancing the kinetic stability with large corona chains. Some attractive interaction of block copolymer micelles exists due to the difference in the refractive indices between the core and selectively solvating medium. However, the repulsive interactions of corona chains overwhelm the attractive interaction. The micelles become kinetically stable and practically athermal because the large separation of the core domains by the corona chains makes the attractive interaction much smaller than the fluctuation energy [Fig. 3(a)]. The interparticle interaction between spherical 1,2-PB-PEO diblock copolymer micelles in water calculated using a modified analytical function, initially proposed by Likos *et al.*, shows that the micellar colloids of 1,2-PB-PEO diblock copolymer chains ($M_n = 6.8$ kg/mol and $f_{PEO} = 0.70$) are sufficiently elastic to form FCC [Fig. 3(b)] [78,88,89]. We observed that the 1,2-PB-PEO micelles initially form metastable HCP and RHCP, while the crystal domains are small in the nucleation and growth process before stable FCC forms by the growth of crystal domains [90]. This strongly suggests that the FCC phase of the 1,2-PB-PEO micellar colloids is driven by the entropic advantage of FCC lattices, as observed from hard-sphere colloids [27].

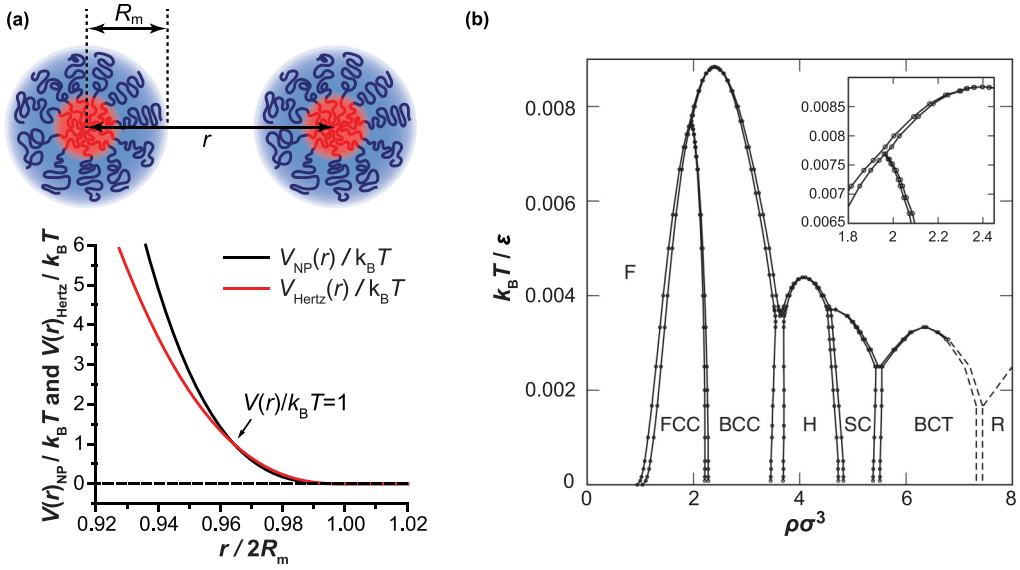

FIG. 3. Evaluation of the elasticity of 1,2-PB-PEO diblock copolymer ($M_n = 6.8$ kg/mol and $f_{PEO} = 0.70$) micelles. (a) Interparticle potential of 1,2-PB-PEO micelles in water $V(r)_{NP}$, calculated using the modified analytical intermicellar potential function proposed by Likos *et al.*, where r is the center-to-center micellar distance and R_m is the radius of the micelles [88]. The repulsive potential $V(r)_{NP}$ is translated to the Hertzian potential $V(r)_{Hertz} = \varepsilon(1 - r/\sigma)^{5/2}$ for $r < \sigma$ and 0 for $r \geqslant \sigma$, where ε is the repulsion energy scale and $\sigma = 2R_m$ is the length scale. The calculated V_{NP} is translated to $\varepsilon = 4 \times 10^3\, k_BT$ for $V_{NP}\,(0.964 \cdot 2R_m)/k_BT = V_{Hertz}(0.964 \times 2R_m)/k_BT = 1$. Copyright 2023 Royal Society of Chemistry (Ref. [78]). (b) Phase diagram of Hertzian spheres. ρ is the number density of spheres. The $k_BT/\varepsilon = 2.5 \times 10^{-4}$ of 1,2-PB-PEO micelles is sufficiently low, i.e., highly elastic, and can form face-centered cubic (FCC) next to the fluid phase (F). Note that the FCC phase domain disappears for the low elasticity spheres of k_BT/ε approximately $>7.5 \times 10^{-3}$. The H, SC, BCT, and R represent hexagonal, simple cubic, body-centered tetragonal, rhombohedral structures. Copyright 2009 American Institute of Physics (Ref. [89]).

The entropic preference for FCC lattices in close-packed structures is universal. However, the non-FCC close-packed structures in block copolymer micelles observed, such as HCP, suggest that a particular energetic advantage outweighs the FCC lattice preference [70]. For hard spheres, calculation showed that HCP lattices are more stable than FCC if lattices are strained [91]. For the HCP structures of block copolymers induced by thermotropic processes under a static environment, such lattice strain is likely lacking, and a different justification is required. All close-packed structures have the same volume fraction of spheres and the number of nearest neighbors. However, the configuration of the interstitial space of close-packed structures changes with the stacking order of 2D-HCP layers. The interstitial space consists of two building units, octahedral and tetrahedral sites [the middle panels of Figs. 4(a) and 4(b)]. The volume of the octahedral site is approximately five times larger than the volume of the tetrahedral one (Fig. S1 in the Supplemental Material (SM) [92]). The interstitial space of FCC is configured as a network of interdigitating octahedral and tetrahedral sites [the right panel of Fig. 4(a)]. In contrast, the interstitial space of HCP has columnar octahedral sites connected by ditetrahedral sites [the right panel of Fig. 4(b)]. Mahynski *et al.* [93,94] investigated the conformational entropy effects of polymer chains in the interstitial space of spheres on FCC or HCP lattices. They found that long polymer chains residing in multiple interstitial sites stabilize HCP because the columnar octahedral space of HCP offers higher conformational freedom to the chains. This finding is directly related to the close-packed structures in block copolymer melts because the chain end-to-end distance of diblock copolymer free chains is larger than the diameter of an inscribable sphere diameter in the octahedral interstitial site by approximately $(\sqrt{2}-1)^{-1} \approx 2.4$ [53,61,77]. For block copolymer micelles in low molecular weight solvents, the conformation effect likely arises from the corona chains longer than the average length [78]. Even polymer chains prepared using a controlled polymerization for narrow molecular weight distributions are sufficiently polydisperse, and relatively long corona chains can serve as the chains residing in multiple interstitial spaces to stabilize the HCP lattices.

The competing lattice configurational entropy for FCC and the chain conformational entropy for HCP suggest that stable RHCP orders may be possible regardless of the size of crystal domains if those contributions are adjusted to be equal and the fluctuation effect pronounces in the stacking order of 2D-HCP layers. The stability of RHCP structures was suggested by a Landau analysis [95]. However, experimental verification was not sought because many RHCP orders observed in diffusive and displacive phase transformations are transitional and eventually become one of the polytypes with regular lattices such as FCC and HCP [27,96]. However, our recent documentation on the close-packed structures of strongly segregated 1,2-PB-PEO micelles in water supports the stability of RHCP orders (Fig. 5) [78]. In that work, close-packed structures of 1,2-PB-PEO micelles were induced by temperature quenching, and the average stacking probability of close-packed structures $\bar{\alpha}$, which is the number average of the stacking probability of 2D-HCP layers in the crystal grains of close-packed structures, was extracted from experimentally

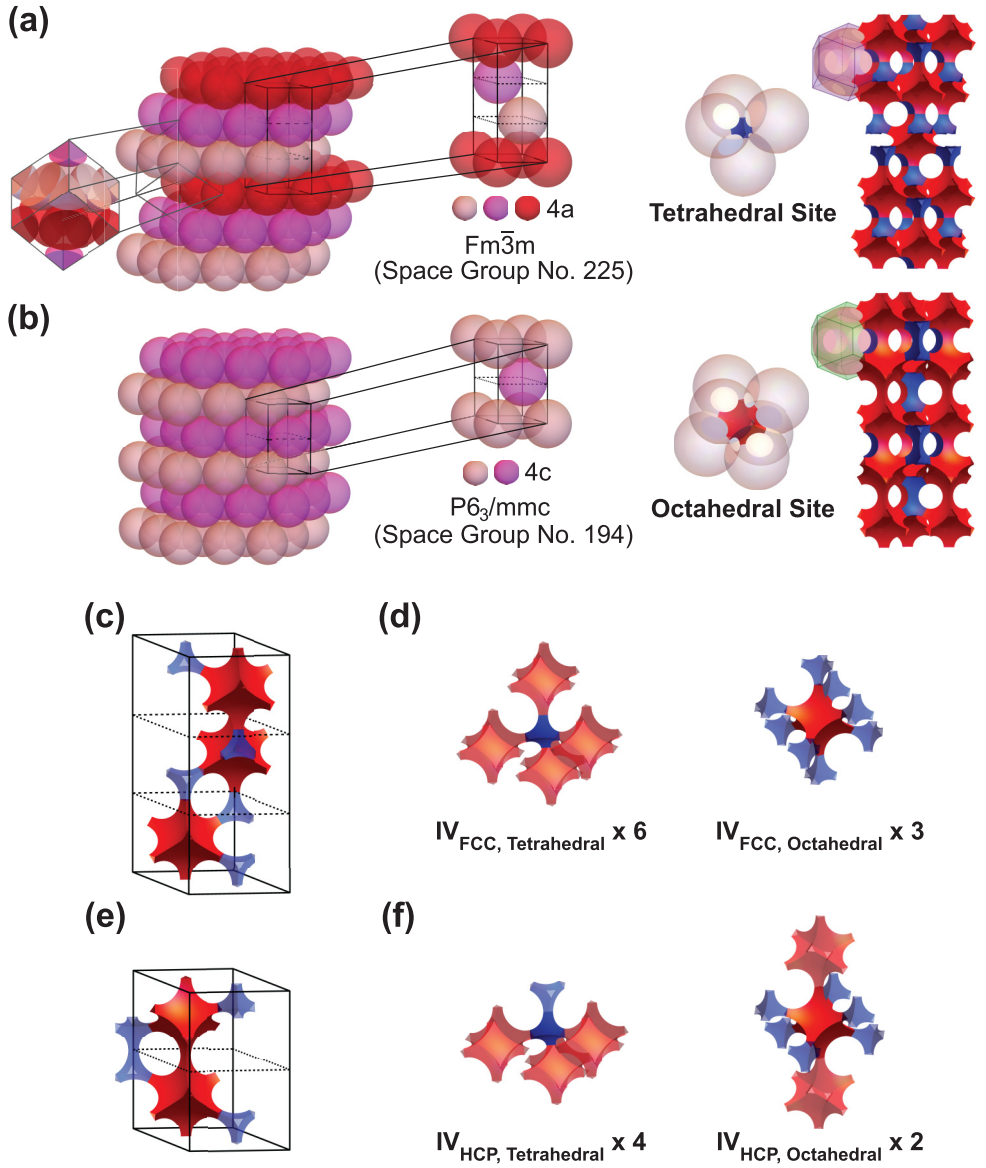

FIG. 4. Spheres on the face-centered cubic (FCC) and hexagonal close-packed (HCP) lattice groups and their interstitial space representation. The tetrahedral and octahedral interstitial spaces are shown in the top middle. For visual convenience, the interstitial spaces shown are by slightly faceted spheres by compression. The interstitial space by nonfaceted spheres in contacts are presented in Fig. S2 in the Supplemental Material (SM) [92]. (a) Stacked two-dimensional (2D) HCP layers forming FCC. The cubic unit cell and the hexagonal unit cell of the stacked 2D-HCP layers are shown. (b) Stacked 2D-HCP layers forming HCP. The hexagonal unit cell is shown. The interstitial spaces by tetrahedral packing and octahedral packing of spheres are presented. The interstitial space networks of FCC and HCP are shown on the right. (c) Interstitial space of FCC in a hexagonal unit cell. (d) Configurations of interstitial spaces ($IV_{FCC, Tetrahedral or Octahedral}$) and the relative populations in a hexagonal unit cell of FCC. (e) Interstitial space of HCP in a hexagonal unit cell. (f) Configurations of interstitial spaces ($IV_{HCP, Tetrahedral or Octahedral}$) and the relative populations in a hexagonal unit cell of HCP.

obtained small angle x-ray scattering intensity profiles. The stacking probability $\alpha = 1$ for a layer of the stacking configuration of "c" and $\alpha = 0$ for "h" (Fig. 1). A perfect FCC crystal domain has $\bar{\alpha} = 1$, perfect HCP $\bar{\alpha} = 0$, and RHCP of equal stacking of "c" and "h" $\bar{\alpha} = 0.5$. Near the fluid-solid phase boundary, $\bar{\alpha}$ is found $\sim$1 (FCC), but as the weight fraction of 1,2-PB-PEO (the number density of micelles) increases, the interstitial space shrinks, and $\bar{\alpha}$ gradually decreases to 0 (HCP). The stability of those close-packed structure crystal grains was tested with the crystal growth as the preference for FCC strengthens with the size of crystals [26]. Growing the crystal grains significantly shifts the stacking probabilities of the close-packed structures of the 1,2-PB-PEO colloids, but the RHCP crystals with $\bar{\alpha} \approx 0.5$ remain nearly unchanged [Figs. 5(c) and 5(d)]. This supports the stability of RHCP.

VIII. APERIODICITY OF RHCP CRYSTAL LATTICES

The International Union of Crystallography (IUCr) defines a crystal as "any solid having an essentially discrete

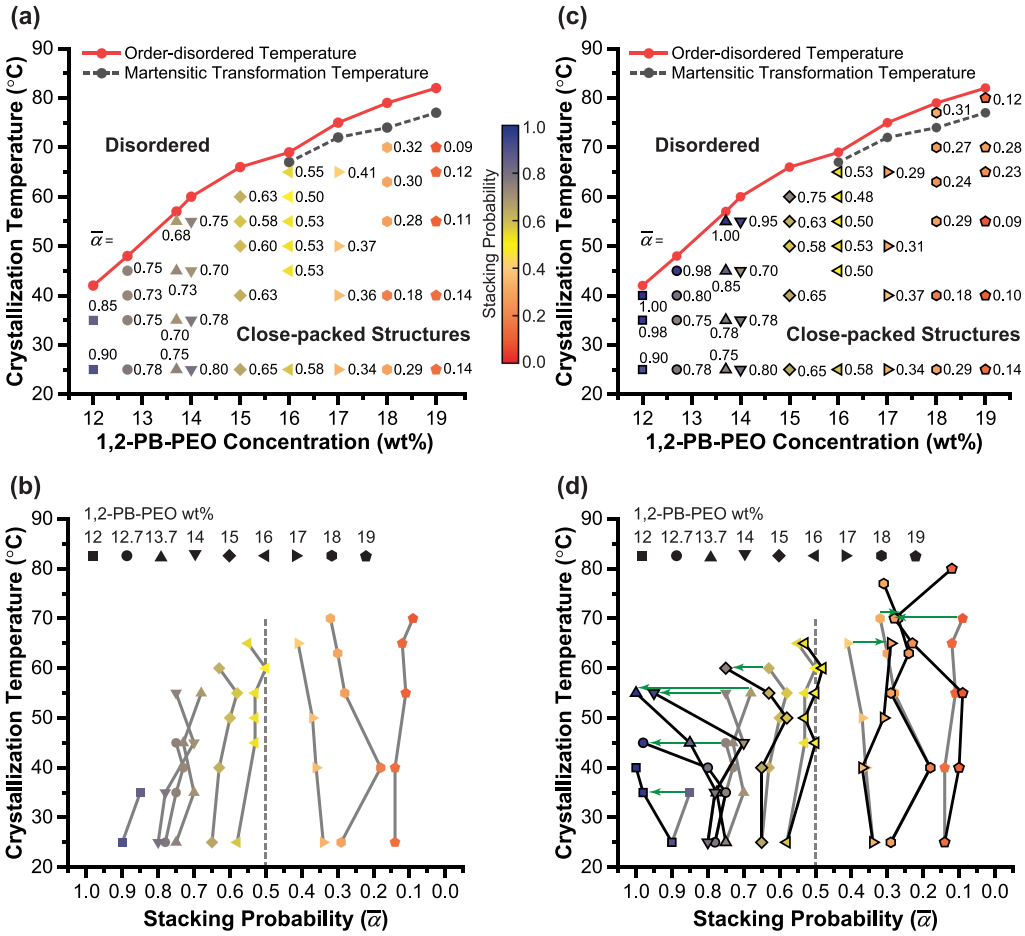

FIG. 5. Stacking probability ($\bar{\alpha}$) diagrams of close-packed structures formed by the micellar colloids of 1,2-PB-PEO diblock copolymer ($M_n = 6.8$ kg/mol and $f_{PEO} = 0.70$) dispersed in water. (a) The $\bar{\alpha}$ of close-packed 1,2-PB-PEO colloids at the crystallization temperature induced by temperature-quenching (30 °C/min) from disordered states over the concentration phase space. (b) Replot of (a) over the $\bar{\alpha}$ space. (c) The $\bar{\alpha}$ of the close-packed crystal grains of 1,2-PB-PEO colloids grown by slow cooling (2–3 °C/min) from the crystallization (nucleation) temperatures to 25 °C. (d) Replot of (c) overlaid with (b). Representative shifts of $\bar{\alpha}$ by the crystal growths are marked with arrows. The crystal growth shifts the $\bar{\alpha}$'s, but the $\bar{\alpha}$'s of the random stacking of hexagonal close-packed (RHCP) structures with $\bar{\alpha} \approx 0.50$ stay nearly the same. Copyright 2023 Royal Society of Chemistry (Ref. [78]).

diffraction diagram" [97]. The RHCP structure generates discrete Bragg diffractions, which qualify RHCP as a crystal but not a periodic crystal because the irregular stacking of 2D-HCP layers forms a set of directionally correlated but irregularly spaced lattices. Those irregular lattices form the Bragg rods (Fig. 6). Bragg rods have undulating intensity profiles in the reciprocal line spaces of noninteger $(h - k)/3$ along the l direction, where h and k are the integral indices of the Miller-Bravais system [98].

RHCP is an *aperiodic crystal* by the IUCr definition, "any crystal in which 3D periodicity can be considered to be absent." However, RHCP does not fit in a subclass of aperiodic crystals [99]. Aperiodic crystals include quasicrystals and incommensurate crystals of modulated, composite, and magnetic structures. The definition of quasicrystals is "an aperiodic crystal with diffraction peaks that may be indexed by n integral indices, where n is a finite number, larger than the dimension of the space" regardless of the existence of a forbidden symmetry such as fivefold rotation [100]. The continuous Bragg rods for RHCP cannot be described with a finite number of integral indices. RHCP is not a quasicrystal. The other class of aperiodic crystals is the incommensurate class, characterized by "Bragg reflection peaks in the diffraction pattern that are well separated but do not belong to a lattice and cannot be indexed by three integer indices" [101]. Since the reflection signatures in the Bragg rods are continuous, RHCP is not an incommensurate crystal. Interestingly, the diffraction patterns of RHCP are qualitatively close to those of random tiling containing discrete reflections and diffuse diffraction signatures from their structural disorders, like the scattering signatures of the RHCP Bragg reflection peaks and rods [102]. RHCP is an aperiodic crystal with a set of lattices directionally correlated but irregularly spaced.

IX. INTERSTITIAL SPACE DISTRIBUTION FACTOR

The stabilization of HCP polytype by polymer chains in the interstitial space proposed by Mahynski *et al.* [93,94] and recent experimental reports on stable HCP and RHCP structures in block copolymer micellar colloids indicate the

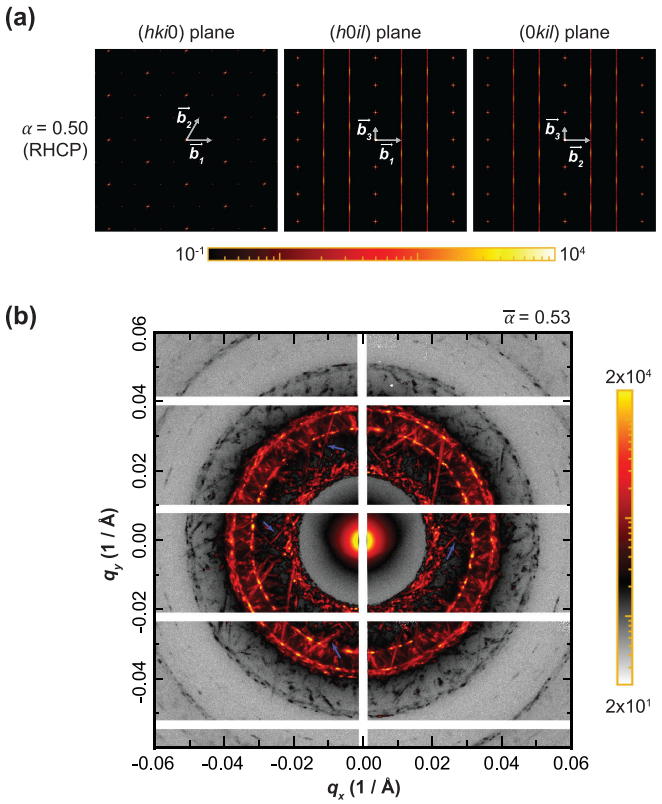

FIG. 6. Reciprocal space representations of the random stacking of hexagonal close-packed (RHCP) structures. (a) Simulated interference patterns of a RHCP crystal ($\alpha = 0.50$) in three planes specified by the Miller-Bravais indices noted above. Bragg rods appear in the ($h0il$) and ($0kil$) planes. (b) Experimental two-dimensional (2D) small angle x-ray scattering (SAXS) pattern of RHCP crystals obtained from 1,2-PB-PEO diblock copolymer ($M_n = 6.8$ kg/mol and $f_{PEO} = 0.70$) micellar colloids dispersed in water (16 wt.%) at 25 °C. The colloids were crystallized at 50 °C from a disordered state by temperature quenching and then slowly cooled to 25 °C (2–3 °C/min) for crystal growth. The polygrain texture of the 2D-SAXS pattern reveals the Bragg rods (some are marked with blue arrows) and reflection peaks. The stacking probability of the close-packed structure crystal grains extracted from the scattering pattern $\bar{\alpha} = 0.53$.

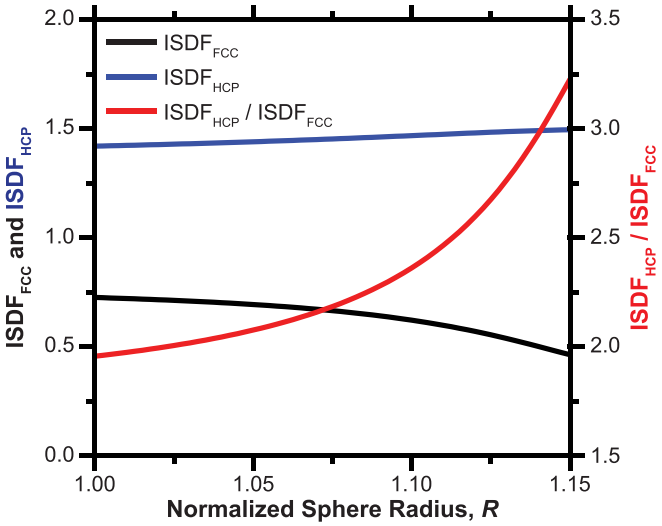

FIG. 7. Interstitial space distribution factors (ISDFs) calculated for face-centered cubic (FCC) and hexagonal close-packed (HCP) polytypes of equal spheres over the normalized sphere radius R to the lattice size $\mathrm{ISDF_{FCC}}$ and $\mathrm{ISDF_{HCP}}$, respectively. As the normalized sphere size increases from $R = 1$, in which the spheres are in contact, the spheres are faceted, and the interstitial space shrinks. The $\mathrm{ISDF_{HCP}/ISDF_{FCC}} > 1$ and increases with R, which indicates the HCP polytype becomes more preferred for polymer chains residing over multiple interstitial sites.

critical role of interstitial space as a crystal structure director [61,62,74,78]. In the close-packed structures of equal spheres, a change in the stacking orders of the 2D-HCP layers results in different crystal structures, as exampled in Fig. 1 and Table I, and the configuration of the interstitial spaces, as also exampled in Fig. 5.

We introduce an interstitial space distribution factor (ISDF) for semiquantitative evaluation of the interstitial space configuration effect on the stabilization of a polytype compared with others in the same polytypic crystal system, i.e., the same particle volume fraction and particle constituents. The ISDF is configured to provide a higher value for the polytype with a layer-stacking configuration that groups larger interstitial sites as the nearest sites around a center site. An ideal (athermal) particle placed in an interstitial space performs random walks, i.e., the conformation of a Gaussian chain, and the translational partition function of a single particle is proportional to the volume, which we assume to be the sum of the volume of the interstitial sites in which the particle is placed and the volume of the nearest interstitial sites, i.e., $IV_i + \sum_{j=1}^{N_{IV,i}} IV_{i,j}$ where IV_i is the volume of the ith interstitial site in which an ideal particle is placed, $IV_{i,j}$ is the volume of the jth nearest interstitial site around the ith site, and $N_{IV,i}$ is the number of the nearest interstitial sites. For a tetrahedral interstitial site in a close-packed structure of equal spheres, $N_{IV,i} = 4$, and for an octahedral site, $N_{IV,i} = 8$ [Figs. 4(d) and 4(f)]. The ISDF includes the probability of placing an ideal particle in an interstitial site differentiated by the volume fraction of the site $f_i = IV_i / \sum_{i=1}^{N_{IV}} IV_i$, where N_{IV} is the number of interstitial sites in a hexagonal unit cell [Figs. 4(c) and 4(e)] or the whole crystal domain if a regular unit cell does not exist. Including the normalization by the interstitial space volume, we define

$$\mathrm{ISDF} = \frac{\sum_{i=1}^{N_{IV}} f_i\left(IV_i + \sum_{j=1}^{N_{IV,i}} IV_{i,j}\right)}{\sum_{i=1}^{N_{IV}} IV_i} = \frac{\sum_{i=1}^{N_{IV}} IV_i\left(IV_i + \sum_{j=1}^{N_{IV,i}} IV_{i,j}\right)}{\left(\sum_{i=1}^{N_{IV}} IV_i\right)^2}.$$

Figure 7 summarizes the ISDFs of FCC and HCP structures of equal spheres ($\mathrm{ISDF_{FCC}}$ and $\mathrm{ISDF_{HCP}}$) over the normalized sphere radius R. The spheres are in contact at $R = 1$. As the sphere radius increases, the spheres become faceted, the interstitial spaces shrink, and the difference in the relative volumes of tetrahedral and octahedral sites increases (Fig. S1 in the SM [92]). The calculated $\mathrm{ISDF_{HCP}}$ is always larger than $\mathrm{ISDF_{FCC}}$ over R, and the $\mathrm{ISDF_{HCP}/ISDF_{FCC}}$ ratio increases as the space of interstitial sites decreases. This result aligns with the increase of the HCP stacking layers in the

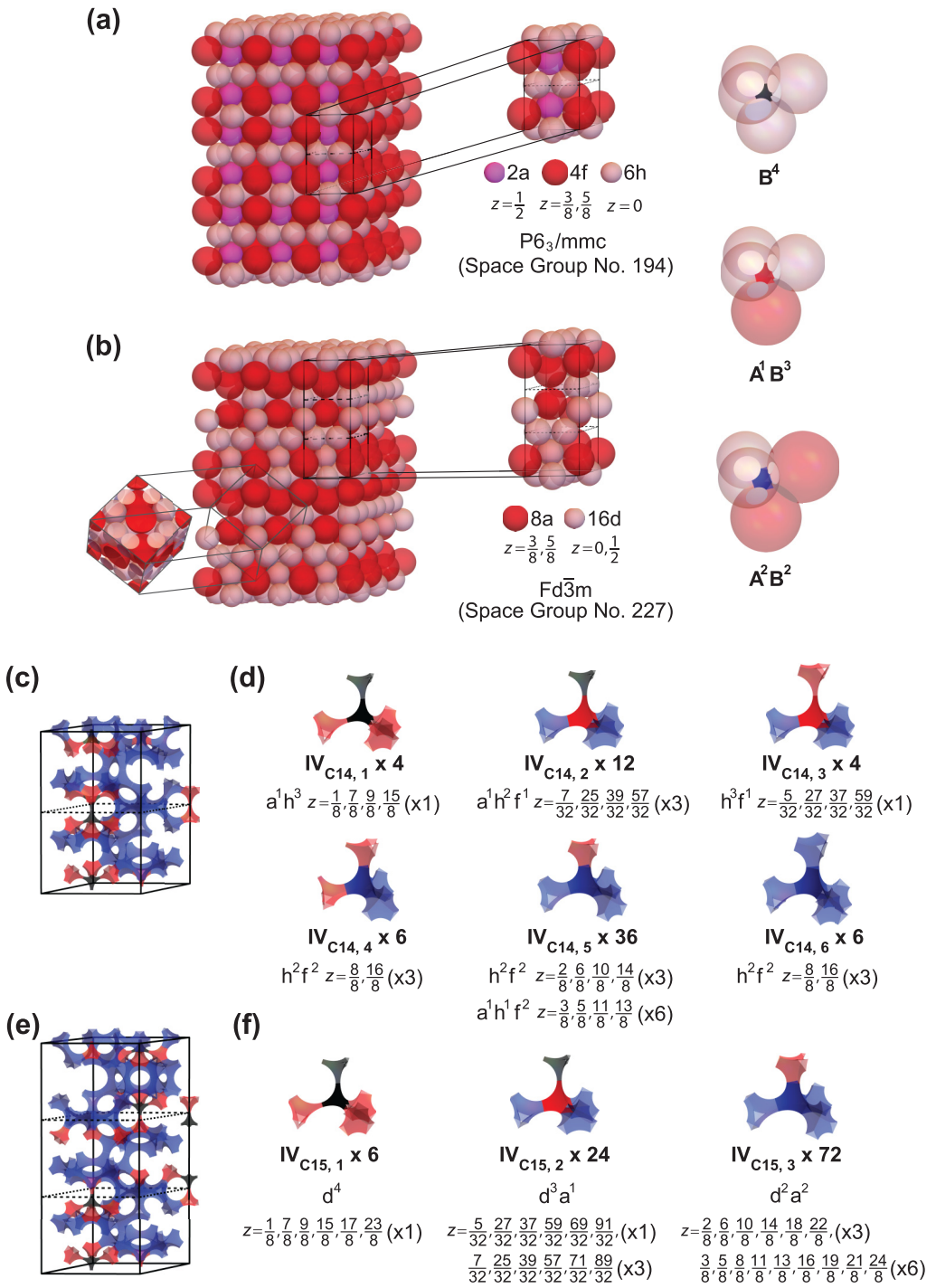

FIG. 8. Spheres on the C14 and C15 phase lattices and their interstitial space representations. Three distinct interstitial spaces by tetrahedrally packed spheres are shown on the right. For visual convenience, the interstitial spaces shown are by slightly faceted spheres by compression. The interstitial spaces by nonfaceted spheres in contact are presented in Fig. S5 in the Supplemental Material (SM) [92,107]. (a) Spheres on the lattices of the C14 phase. The hexagonal unit cell, Wyckoff positions, and symmetry group are presented. (b) Spheres on the lattices of the C15 phase with the cubic and hexagonal unit cells. The superscripts of A and B under the tetrahedrally close-packed spheres on the right note the number of sphere species forming an interstitial site. (c) Interstitial space network in a hexagonal unit cell of C14 phase. (d) Tetrahedral interstitial site clusters of different site configurations in a hexagonal unit cell of the C14 phase. The population of each interstitial space, Wyckoff notations of the lattices forming each interstitial space, the number of lattices in superscripts, and the z positions of interstitial space are noted. (e) Interstitial network in a hexagonal unit cell of the C15 phase. (f) Tetrahedral interstitial site clusters of different site configurations in a hexagonal unit cell of the C15 phase.

close-packed structures of 1,2-PB-PEO micellar colloids in water by increasing the colloid weight fraction, i.e., a decrease of the stacking probability, shown in Figs. 5(b) and 5(d). At the volume fraction of close-packed colloids where the colloids are in contact and with the largest interstitial space, the entropic preference for HCP by the conformational entropy of corona chains is the least against the configurationally preferred FCC lattices. As the size of spheres increases, i.e., the unit cell lattices decrease, the interstitial sites shrink, and the chain conformation entropy for HCP lattices pronounces and gradually overcomes the FCC preference.

We also evaluated the ISDFs of the C14 and C15 Laves phases, which are structurally equivalent to the HCP and FCC of equal spheres [75,76]. Laves phases have binary compositions AB_2, and their crystal structures are determined by the stacking orders of the 2D-HCP layers of A or B on a kagome lattice [24,103]. The C14 and C15 phases are often referred to as the $MgZn_2$ and $MgCu_2$ structures, respectively, after the binary intermetallic alloys forming those structures and have been observed from colloidal systems [104,105]. The 2D-HCP layers of Laves phases have three registration lattice groups available for layer stacking, which makes the construction of Laves phases equivalent to the ABC layer stacking of close-packed structures of equal spheres [106]. The structural equivalency of the C14 and C15 phases to the HCP and FCC originates from two different registration lattice groups at $z = \frac{1}{2}$ available for a 2D-HCP layer of B, which is equivalent to the two registration lattice groups on a 2D-HCP layer of equal spheres for the next 2D-HCP layer, forming the ABC stacking of FCC or the AB stacking of HCP by choice of registration site group.

Figure 8 describes the crystal structures and interstitial spaces of the C14 and C15 structures. The radius of sphere A is larger than the radius of sphere B by $\sqrt{3/2}$. The C14 and C15 structures have three distinct tetrahedral interstitial sites by four B spheres (B^4), one A and three B (A^1B^3), and two A and two B (A^2B^2), where the letters and superscripts indicate the sphere species and the number of spheres (the top right of Fig. 8). Those tetrahedral interstitial sites have four nearest sites. In a unit cell of C14, six tetrahedral interstitial site clusters of different site configurations are formed, as shown in Fig. 8(d). The population of the tetrahedral interstitial site clusters in a hexagonal unit cell, packing environments by lattice Wyckoff notations, the number of those lattices as superscripts, and the z positions are provided below each interstitial site cluster representation. In a unit cell of C15, three different tetrahedral interstitial site clusters configure the network, as shown in Fig. 8(f).

The C14 structure forms a more diverse array of tetrahedral interstitial site clusters. The $IV_{C14,6}$ cluster of the center site by A^2B^2 and the four nearest sites also by A^2B^2 has the largest volume in the interstitial sites in the Laves phases. The largest tetrahedral interstitial site group in a hexagonal unit cell of C15 is $IV_{C15,3}$ of the center site by A^2B^2, one nearest site by A^1B^3, and three nearest sites by A^2B^2. The smallest tetrahedral interstitial site clusters in C14 and C15 structures are $IV_{C14,1}$ and $IV_{C15,1}$, of which configurations are the same. Those clusters have the same center site by B^4, one nearest site by B^4, and three nearest sites by A^1B^3. As the radius of spheres increases and the spheres become faceted, the difference in the volumes of those tetrahedral interstitial sites increases, as shown in Fig. S4 in the SM [92].

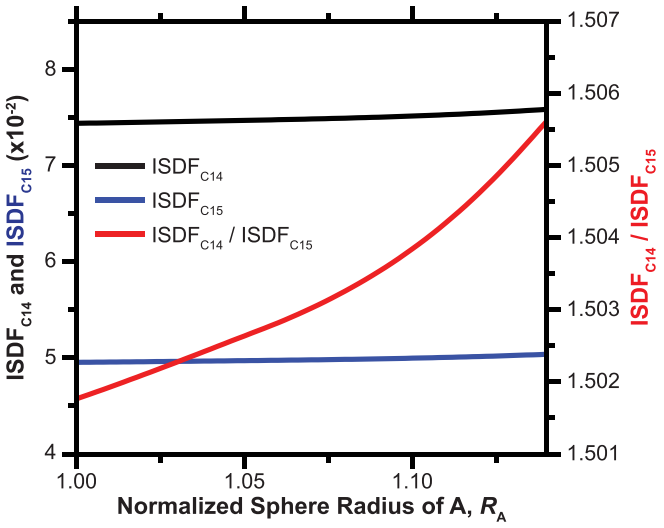

FIG. 9. Interstitial space distribution factors (ISDFs) calculated for C14 and C15 structures over the normalized radius of sphere A, $R_A = \sqrt{3/2}R_B$, to the lattice size. As the normalized sphere radius increases from $R_A = 1$ in which the spheres are in contact, the spheres are faceted, and the interstitial space shrinks. The relative ISDF of C14 over C15, $ISDF_{C14}/ISDF_{C15}$, is >1 and increases as R_A increases. The C14 polytype becomes a more preferred structure for polymer chains residing over multiple interstitial sites because of the larger conformational entropy.

Figure 9 summarizes the ISDFs of C14 and C15 ($ISDF_{C14}$ and $ISDF_{C15}$) and their ratio. The $ISDF_{C14}$ is ~50% larger than the $ISDF_{C15}$ over the normalized sphere radius of A, R_A, and this ratio slightly increases as the normalized radii of A and B spheres of $R_A = \sqrt{3/2}\,R_B$ increase. If the C15 structure is more stable than C14 because of the lattice configurational entropy as in FCC, we expect that the addition of long polymer chains to the interstitial space of Laves phases will stabilize the C14 phase and the random stacking of Laves phase layers, which are structurally equivalent to HCP and RHCP of equal spheres, respectively. This hypothesis should be testable using the alloys of strongly segregated block copolymer micellar colloids.

X. QUESTIONS

So far, the FCC, RHCP, and HCP polytypes of block copolymer colloids have been identified as stable close-packed structures. However, the stability of other polytypes with a regular stacking order of 2D-HCP layers, as some examples are shown in Fig. 1 and Table I, needs to be tested. The same question also applies to the Laves phases of block copolymer colloids if those phases are located. As a relevant example, silicon carbides are known to form more than 200 polytypes [108]. Another question is whether interstitial space engineering using polymer chains is extendable to other superlattices and quasicrystals [13,109–111].

XI. BLOCK COPOLYMER AS MODEL MATERIALS FOR UNIVERSALITY OF LONG-RANGE ORDERED STRUCTURES

The chemical inhomogeneity of block copolymer chains offers rich structural and physical phenomena, which have been a major interest in polymer science and engineering, materials research, chemistry, and physics. Block copolymer chains form partitioning interfaces to segregate chemically incompatible polymer domains, and the preferred curvature and elasticity of the interface are freely adjustable by tailoring the molecular architectures and chemical compositions [31,54]. The segregated domains self-assemble into long-range ordered structures, often of which crystallographic symmetry and morphology are the same or closely related to the structures in other systems, for example, elements, surfactants, and even the internal structures of neutron stars [30,112–114]. However, among those seemingly universal structures, close-packed structures have been regarded as a peripheral problem in block copolymer systems until the recent discoveries of polytypes of spherical domains [61,62,77,78]. Those polytypes reiterate that block copolymers are highly versatile systems capable of leveraging geometrical components for target self-assembly, such as excluded volume, interstitial space, and particle interface sphericity [4,17,78,93]. For example, strongly segregated block copolymer micelles can serve as athermal model spherical colloids with high tunability. Adding a small number of long corona chains to block copolymer micelles will increase the interstitial space effect that may initiate transformations to other polytypes or structures. The degree of solvent selectivity tunes the energy scale in the particle deformation, i.e., sphericity, for the selection of packing structures. The discovery of packing structures in block copolymer materials and relevant physics will continue.

ACKNOWLEDGMENTS

In this paper, we used resources of the 12-ID beamline of the National Synchrotron Light Source II, a U.S. Department of Energy (DOE) Office of Science User Facility operated for the DOE Office of Science by Brookhaven National Laboratory under Contract No. DESC0012704. L.C. is supported by the Shanghai Sailing Program (22YF1430500).

[1] J. N. Israelachvili, *Intermolecular and Surface Forces*, 3rd ed. (Academic Press, Waltham, 2011).
[2] H. S. Lee, M. Adhimoolam Arunagirinathan, A. Vagias, S. Lee, J. R. Bellare, H. T. Davis, E. W. Kaler, A. V. McCormick, and F. S. Bates, Langmuir **30**, 12743 (2014).
[3] V. S. K. Balagurusamy, G. Ungar, V. Percec, and G. Johansson, J. Am. Chem. Soc. **119**, 1539 (1997).
[4] S. Lee, C. Leighton, and F. S. Bates, Proc. Natl. Acad. Sci. USA **111**, 17723 (2014).
[5] J. G. Gay and B. J. Berne, J. Chem. Phys. **74**, 3316 (1981).
[6] P. F. Damasceno, M. Engel, and S. C. Glotzer, Science **337**, 453 (2012).
[7] S. A. Kim, K.-J. Jeong, A. Yethiraj, and M. K. Mahanthappa, Proc. Natl. Acad. Sci. USA **114**, 4072 (2017).
[8] G. Ungar, Y. Liu, X. Zeng, V. Percec, and W.-D. Cho, Science **299**, 1208 (2003).
[9] X. Zeng, G. Ungar, Y. Liu, V. Percec, A. E. Dulcey, and J. K. Hobbs, Nature (London) **428**, 157 (2004).
[10] Y. Liu, T. Liu, X.-Y. Yan, Q.-Y. Guo, H. Lei, Z. Huang, R. Zhang, Y. Wang, J. Wang, F. Liu *et al.*, Proc. Natl. Acad. Sci. USA **119**, e2115304119 (2022).
[11] S. Lee, M. J. Bluemle, and F. S. Bates, Science **330**, 349 (2010).
[12] K. Kim, M. W. Schulze, A. Arora, R. M. Lewis, M. A. Hillmyer, K. D. Dorfman, and F. S. Bates, Science **356**, 520 (2017).
[13] J. Zhang and F. S. Bates, J. Am. Chem. Soc. **134**, 7636 (2012).
[14] C. R. Iacovella, A. S. Keys, and S. C. Glotzer, Proc. Natl. Acad. Sci. USA **108**, 20935 (2011).
[15] T. C. Hales, Ann. Math. **162**, 1065 (2005).
[16] W. G. Hoover, D. A. Young, and R. Grover, J. Chem. Phys. **56**, 2207 (1972).
[17] D. Frenkel, Nat. Mater. **14**, 9 (2014).
[18] L. Onsager, Ann. NY Acad. Sci. **51**, 627 (1949).
[19] W. W. Wood and J. D. Jacobson, J. Chem. Phys. **27**, 1207 (1957).
[20] B. J. Alder and T. E. Wainwright, J. Chem. Phys. **27**, 1208 (1957).
[21] P. N. Pusey and W. van Megen, Nature (London) **320**, 340 (1986).
[22] L. S. Ramsdell, Am. Mineralog. **32**, 64 (1947).
[23] R. J. Angel, Z. Krist. Cryst. Mater. **176**, 193 (1986).
[24] F. C. Frank and J. S. Kasper, Acta Cryst. **12**, 483 (1959).
[25] P. G. Bolhuis, D. Frenkel, S.-C. Mau, and D. A. Huse, Nature (London) **388**, 235 (1997).
[26] S.-C. Mau and D. A. Huse, Phys. Rev. E **59**, 4396 (1999).
[27] V. C. Martelozzo, A. B. Schofield, W. C. K. Poon, and P. N. Pusey, Phys. Rev. E **66**, 021408 (2002).
[28] S. Pronk and D. Frenkel, J. Chem. Phys. **110**, 4589 (1999).
[29] V. Abetz and P. Simon, Adv. Polym. Sci. **189**, 125 (2005).
[30] L. Leibler, Macromolecules **13**, 1602 (1980).
[31] F. S. Bates, M. A. Hillmyer, T. P. Lodge, C. M. Bates, K. T. Delaney, and G. H. Fredrickson, Science **336**, 434 (2012).
[32] X. Cheng, L. Lin, W. E, P. Zhang, and A.-C. Shi, Phys. Rev. Lett. **104**, 148301 (2010).
[33] T. P. Lodge and M. C. Dalvi, Phys. Rev. Lett. **75**, 657 (1995).
[34] C. Creton, G. Hu, F. Deplace, L. Morgret, and K. R. Shull, Macromolecules **42**, 7605 (2009).
[35] M. S. Dimitriyev, A. Reddy, and G. M. Grason, Macromolecules **56**, 7184 (2023).
[36] M. Goswami, O. O. Iyiola, W. Lu, K. Hong, P. Zolnierczuk, L.-R. Stingaciu, W. T. Heller, O. Taleb, B. G. Sumpter, and D. T. Hallinan, Jr., Macromolecules **56**, 762 (2023).
[37] J. Xie and A.-C. Shi, Langmuir **39**, 11491 (2023).
[38] L. Tsaur and U. B. Wiesner, Polymers **15**, 2020 (2023).
[39] M. W. Matsen, J. Phys.: Condens. Matter **14**, R21 (2002).

[40] M. W. Matsen and F. S. Bates, Macromolecules **29**, 7641 (1996).

[41] M. Gervais and B. Gallot, Makromol. Chem. **171**, 157 (1973).

[42] M. W. Matsen, Macromolecules **45**, 2161 (2012).

[43] C.-Y. Chang, G.-M. Manesi, C.-Y. Yang, Y.-C. Hung, K.-C. Yang, P.-T. Chiu, A. Avgeropoulos, and R.-M. Ho, Proc. Natl. Acad. Sci. USA **118**, e2022275118 (2021).

[44] A. Reddy, M. B. Buckley, A. Arora, F. S. Bates, K. D. Dorfman, and G. M. Grason, Proc. Natl. Acad. Sci. USA **115**, 10233 (2018).

[45] K. Kim, A. Arora, R. M. Lewis, M. Liu, W. Li, A.-C. Shi, K. D. Dorfman, and F. S. Bates, Proc. Natl. Acad. Sci. USA **115**, 847 (2018).

[46] Y. Liu, H. Lei, Q.-Y. Guo, X. Liu, X. Li, Y. Wu, W. Li, W. Zhang, G. Liu, X.-Y. Yan *et al.*, Chinese J. Polym. Sci. **41**, 607 (2023).

[47] F. S. Bates, R. E. Cohen, and C. V. Berney, Macromolecules **15**, 589 (1982).

[48] R. W. Richards and J. L. Thomason, Macromolecules **16**, 982 (1983).

[49] A. N. Semenov, Macromolecules **22**, 2849 (1989).

[50] M. W. Matsen and F. S. Bates, Macromolecules **29**, 1091 (1996).

[51] E. W. Cochran, C. J. Garcia-Cervera, and G. H. Fredrickson, Macromolecules **39**, 2449 (2006).

[52] M. W. Matsen, Phys. Rev. Lett. **99**, 148304 (2007).

[53] M. W. Matsen, Eur. Phys. J. E **30**, 361 (2009).

[54] N. Xie, W. Li, F. Qiu, and A.-C. Shi, ACS Macro Lett. **3**, 906 (2014).

[55] L. Chen, Y. Qiang, and W. Li, Macromolecules **51**, 9890 (2018).

[56] S. Chanpuriya, K. Kim, J. Zhang, S. Lee, A. Arora, K. D. Dorfman, K. T. Delaney, G. H. Fredrickson, and F. S. Bates, ACS Nano **10**, 4961 (2016).

[57] M. Liu, W. Li, F. Qiu, and A.-C. Shi, Soft Matter **12**, 6412 (2016).

[58] R. Liu, Z. Sun, H. Huang, J. A. Johnson, A. Alexander-Katz, and C. A. Ross, Nano Lett. **23**, 177 (2023).

[59] K. Imaizumi, T. Ono, T. Kota, S. Okamoto, and S. Sakurai, J. Appl. Crystallogr. **36**, 976 (2003).

[60] Y.-Y. Huang, J.-Y. Hsu, H.-L. Chen, and T. Hashimoto, Macromolecules **40**, 406 (2007).

[61] N.-W. Hsu, B. Nouri, L.-T. Chen, and H.-L. Chen, Macromolecules **53**, 9665 (2020).

[62] C. Zhang, D. L. Vigil, D. Sun, M. W. Bates, T. Loman, E. A. Murphy, S. M. Barbon, J.-A. Song, B. Yu, G. H. Fredrickson *et al.*, J. Am. Chem. Soc. **143**, 14106 (2021).

[63] E. Helfand and Z. R. Wasserman, in *Developments in Block Copolymers—1*, edited by I. Goodman (Applied Science, New York, 1982), pp. 99.

[64] A. S. Keys and S. C. Glotzer, Phys. Rev. Lett. **99**, 235503 (2007).

[65] E. G. Kelley, T. P. Smart, A. J. Jackson, M. O. Sullivan, and T. H. Epps, Soft Matter **7**, 7094 (2011).

[66] A.-P. Hynninen and M. Dijkstra, Phys. Rev. E **68**, 021407 (2003).

[67] M. Watzlawek, C. N. Likos, and H. Löwen, Phys. Rev. Lett. **82**, 5289 (1999).

[68] G. M. Grason, J. Chem. Phys. **126**, 114904 (2007).

[69] I. W. Hamley, J. A. Pople, and O. Diat, Colloid. Polym. Sci. **276**, 446 (1998).

[70] M. J. Park, J. Bang, T. Harada, K. Char, and T. P. Lodge, Macromolecules **37**, 9064 (2004).

[71] M. J. Park, K. Char, J. Bang, and T. P. Lodge, Langmuir **21**, 1403 (2005).

[72] M. W. Matsen, Macromolecules **28**, 5765 (1995).

[73] M. W. Matsen, Phys. Rev. Lett. **74**, 4225 (1995).

[74] L.-T. Chen, C.-Y. Chen, and H.-L. Chen, Polymer **169**, 131 (2019).

[75] A. J. Mueller, A. P. Lindsay, A. Jayaraman, S. Weigand, T. P. Lodge, M. K. Mahanthappa, and F. S. Bates, Macromolecules **55**, 8332 (2022).

[76] A. P. Lindsay, G. K. Cheong, A. J. Peterson, S. Weigand, K. D. Dorfman, T. P. Lodge, and F. S. Bates, Macromolecules **54**, 7088 (2021).

[77] L.-T. Chen, Y.-T. Huang, C.-Y. Chen, M.-Z. Chen, and H.-L. Chen, Macromolecules **54**, 8936 (2021).

[78] J. Ahn, L. Chen, P. T. Underhill, G. Freychet, M. Zhernenkov, and S. Lee, Soft Matter **19**, 3257 (2023).

[79] O. S. Edwards and H. Lipson, Proc. R. Soc. Lond. A **180**, 268 (1942).

[80] H. Cynn, C. S. Yoo, B. Baer, V. Iota-Herbei, A. K. McMahan, M. Nicol, and S. Carlson, Phys. Rev. Lett. **86**, 4552 (2001).

[81] A. Niozu, Y. Kumagai, T. N. Hiraki, H. Fukuzawa, K. Motomura, M. Bucher, K. Asa, Y. Sato, Y. Ito, D. You *et al.*, Proc. Natl. Acad. Sci. USA **118**, e2111747118 (2021).

[82] T. L. Malkin, B. J. Murray, A. V. Brukhno, J. Anwar, and C. G. Salzmann, Proc. Natl. Acad. Sci. USA **109**, 1041 (2012).

[83] A. V. Petukhov, I. P. Dolbnya, D. G. A. L. Aarts, G. J. Vroege, and H. N. W. Lekkerkerker, Phys. Rev. Lett. **90**, 028304 (2003).

[84] A. J. Archer, M. C. Walters, U. Thiele, and E. Knobloch, Phys. Rev. E **90**, 042404 (2014).

[85] L. Lupi, A. Hudait, B. Peters, M. Grünwald, R. Gotchy Mullen, A. H. Nguyen, and V. Molinero, Nature (London) **551**, 218 (2017).

[86] W. C. K. Poon, E. R. Weeks, and C. P. Royall, Soft Matter **8**, 21 (2012).

[87] C. P. Royall, W. C. K. Poon, and E. R. Weeks, Soft Matter **9**, 17 (2013).

[88] L. Gury, S. Kamble, D. Parisi, J. Zhang, J. Lee, A. Abdullah, K. Matyjaszewski, M. R. Bockstaller, D. Vlassopoulos, and G. Fytas, Macromolecules **54**, 7234 (2021).

[89] J. C. Pàmies, A. Cacciuto, and D. Frenkel, J. Chem. Phys. **131**, 044514 (2009).

[90] L. Chen, H. S. Lee, and S. Lee, Proc. Natl. Acad. Sci. USA **115**, 7218 (2018).

[91] S. Pronk and D. Frenkel, Phys. Rev. Lett. **90**, 255501 (2003).

[92] See Supplemental Material at http://link.aps.org/supplemental/10.1103/PhysRevMaterials.7.110301 for the visualizations of interstitial spaces of close-packed and Laves phases and the volume changes of the interstitial sites by increasing the sphere radius.

[93] N. A. Mahynski, A. Z. Panagiotopoulos, D. Meng, and S. K. Kumar, Nat. Commun. **5**, 4472 (2014).

[94] N. A. Mahynski, S. K. Kumar, and A. Z. Panagiotopoulos, Soft Matter **11**, 280 (2015).

[95] V. P. Dmitriev, S. B. Rochal, Y. M. Gufan, and P. Tolédano, Phys. Rev. Lett. **62**, 2495 (1989).

[96] S. Auer and D. Frenkel, Nature (London) **409**, 1020 (2001).
[97] International Union of Crystallography, Acta Cryst. A **48**, 922 (1992).
[98] B. E. Warren, *X-Ray Diffraction* (Addison-Wesley, Reading, 1969).
[99] R. Lifshitz, Z. Krist. **222**, 313 (2007).
[100] Online Dictionary of Crystallography, https://dictionary.iucr.org/.
[101] T. Janssen, A. Janner, A. Looijenga-Vos, and P. M. de Wolff, in *International Tables for Crystallography, Volume C: Mathematical, Physical and Chemical Tables*, edited by E. Prince (Springer, Dordrecht, 2006), pp. 907.
[102] M. Baake and M. Höffe, J. Stat. Phys. **99**, 219 (2000).
[103] K. D. Dorfman, Macromolecules **54**, 10251 (2021).
[104] Z. Chen and S. O'Brien, ACS Nano **2**, 1219 (2008).
[105] É. Ducrot, M. He, G.-R. Yi, and D. J. Pine, Nat. Mater. **16**, 652 (2017).
[106] J. Aufrecht, W. Baumann, A. Leineweber, V. Duppel, and E. Mittemeijer, Philos. Mag. **90**, 3149 (2010).
[107] Z. V. Vardeny, A. Nahata, and A. Agrawal, Nat. Photonics **7**, 177 (2013).
[108] R. Cheung, *Silicon Carbide Microelectromechanical Systems for Harsh Environments* (Imperial College Press, London, 2006).
[109] E. V. Shevchenko, D. V. Talapin, N. A. Kotov, S. O'Brien, and C. B. Murray, Nature (London) **439**, 55 (2006).
[110] D. V. Talapin, E. V. Shevchenko, M. I. Bodnarchuk, X. Ye, J. Chen, and C. B. Murray, Nature (London) **461**, 964 (2009).
[111] S. Abbas and T. P. Lodge, Phys. Rev. Lett. **97**, 097803 (2006).
[112] V. Luzzati, A. Tardieu, T. Gulik-Krzywicki, E. Rivas, and F. Reiss-Husson, Nature (London) **220**, 485 (1968).
[113] S. Alexander and J. McTague, Phys. Rev. Lett. **41**, 702 (1978).
[114] J. M. Lattimer and M. Prakash, Science **304**, 536 (2004).